

Effects of Formic Acid Treatment on Properties of Oil Palm Empty Fruit Bunch (OPEFB)-Based All Cellulose Composite (ACC) Films

Nur Liyana Izyan Zailuddin, Azlin Fazlina Osman* and Rozyanty Rahman

Center of Excellence Geopolymer and Green Technology (CEGeoGTech),
School of Materials Engineering, Universiti Malaysia Perlis,
02600 Arau, Perlis, Malaysia

*Corresponding author: azlin@unimap.edu.my

Published online: 30 June 2020

To cite this article: Nur Liyana Izyan Zailuddin, Azlin Fazlina Osman and Rozyanty Rahman (2020). Effects of formic acid treatment on properties of oil palm empty fruit bunch (OPEFB)-based all cellulose composite (ACC) films. *Journal of Engineering Science*, 16(1), 75–95, <https://doi.org/10.21315/jes2020.16.1.6>.

To link to this article: <https://doi.org/10.21315/jes2020.16.1.6>

Abstract: *This study explored the potential of using oil palm empty fruit bunch (OPEFB) in the production all-cellulose composite (ACC) films. The isolation process of the raw OPEFB fibre was carried out using chemical process to extract the OPEFB nanocellulose. The ACC films from the OPEFB nanocellulose and microcrystalline cellulose (MCC) were prepared using dimethylacetamide (DMAC) and lithium chloride LiCl solvent system whereby the partially dissolved cellulose was transformed into the matrix phase surrounding the remaining non-dissolved fibre. The ACC films containing 1%, 2%, 3% and 4% (wt. vol⁻¹) OPEFB cellulose and 3% (wt. vol⁻¹) MCC were prepared and the effects of formic acid as chemical treatment for the OPEFB nanocellulose on tensile properties of the ACC film were investigated. Results indicate that the chemical treatment using formic acid has reduced the hydroxyl group composition in the cellulose, and caused greater dissolution of the cellulose during the formation of the ACC film. As a result, the tensile strength and modulus of elasticity of the ACC film were significantly enhanced. However, both untreated and treated ACC films experienced the reduction in both properties when the cellulose concentration was increased from 1% to 4% (wt. vol⁻¹), due to the saturation of the cellulose particles and non-homogeneity of the ACC system. Findings also suggested that the formic acid-treated ACC film tends to absorb more moisture as compared to the untreated composite films, allowing greater biodegradation rate when buried in soil.*

Keywords: all-cellulose composite, nanocellulose, tensile properties, biodegradability

1. INTRODUCTION

Generally, plastics are perceived as basic or primeval element used extensively in packaging industry due to their low cost, lightweight, ease of manufacturing and shaping.¹ Nowadays, more researches and studies are focusing on the use of biologically degradable composite materials for maintaining ecosystem balance and obtaining other benefits, such as biodegradability, cheap in price and ability to fulfil and balance out the economic interest of companies and industries.¹⁻⁴ Natural composite films from various resources are being investigated to substitute non-biodegradable petrochemical based plastics.¹⁻³ The most known renewable or sustainable materials that are able to produce biodegradable plastics are cellulose and starch.^{1,3,5} Cellulose is widely known as the world's most prevalent biopolymer and their abundance characteristic has raised demand to be used as green and biocompatible products.² Great attentions are drawn towards celluloses for their unique and particular properties like high mechanical strength, renewability, biodegradability, cheap in price as well as good film-forming performance.²

In Malaysia, the plantation of palm oil produces large amount of residues like oil palm empty fruit bunch (OPEFB), oil palm shell and other biomass wastes.⁶ Even though the OPEFB is categorised as lignocelluloses waste, it consists of high percentage of cellulose.^{6,7} OPEFB is usually disposed in landfills, burnt off or composted to organic fertiliser. Burning of these wastes can lead to environmental problems such as air pollution. Several issues regarding the proper management and regulation of these lignocelluloses residues can be resolved by optimally employ these natural resources to its fullest extent. For instance, scientists can investigate and reveal some potential uses of these biomass wastes and modify them in a way that they can be more viable for numerous applications.^{7,8}

The term green composites can be referred to environmental friendly materials with the use of green matrix in addition to natural fibres.⁹ All-cellulose composite (ACC) is one of the green composites being studied extensively in recent works.^{2,6,9} ACC can be described as "single-material composite" or "self-reinforced composite" because it uses the same cellulose source for both the reinforcement and matrix. The main advantage of this composite is that the interface or chemical bonding between the reinforcement and matrix can be improved or enhanced.⁹ ACC can be produced by the process of "surface selective dissolution" of the cellulose materials. This concept can be explained when the surface layer of cellulose is dissolved by the cellulose solvent which is then regenerated to form the matrix domain surrounding the non-dissolved part of the cellulose which remains as the fibre reinforcement of the composite.^{6,9}

Since cellulose is made up of complex structure, it cannot be dissolved in most solvents. Nonetheless, there are some solvents that can facilitate the dissolution process of cellulose such as N, N-dimethyl acetamide/lithium chloride (DMAC/LiCl), N-methylmorpholine N-oxide (NMMO), ionic liquids (ILs) and others. DMAC/LiCl system is thought to be a good solvent for cellulose due to its ability to allow great cellulose-solvent interactions.^{6,10} Therefore, this solvent system is well recognised among researchers and adapted to conform to different types of cellulose sources.¹¹

In this study, the ACC films were produced using nanocellulose derived from the OPEFB. DMAC/LiCl solvent system was used, whereby the partially dissolved cellulose was transformed into the matrix phase surrounding the remaining non-dissolved fibres. The effects of cellulose chemical treatment by formic acid on tensile properties, water absorption and soil biodegradability of the ACC films were studied and reported herein.

2. METHODOLOGY

2.1 Materials

The raw materials used in this study were OPEFB which was used as received from Malaysian Palm Oil Board (MPOB) Bangi, Selangor and microcrystalline cellulose (MCC) from cotton linters (Aldrich Chemistry) with the average size of 51 μm . The chemicals used for the production of ACC films were; sodium hydroxide (NaOH), ethanol ($\text{C}_2\text{H}_5\text{OH}$) and acetone ($\text{C}_3\text{H}_6\text{O}$), which were supplied by HmbG® Chemicals. Sodium chlorite (NaClO_2) was supplied by Sigma-Aldrich (Germany) and was used in the bleaching treatment of the OPEFB fibre. Sulfuric acid was used during the hydrolysis step of OPEFB and has a molar mass of 98.10 g mol^{-1} . Formic acid is a product of PC Laboratory Reagent and was used to treat the nanocellulose. N,N-Dimethylacetamide (DMAC) was also manufactured by Merck, Germany and was used to dissolve the cellulose. Lithium chloride (LiCl) was supplied by Across, Belgium and was used together with DMAC to dissolve the cellulose.

2.2 Chemical Isolation Processes of OPEFB Fibre to Obtain the Nanocellulose

Firstly, the OPEFB fibre was treated in 4% NaOH solution at the temperature of 80°C for 1 h under stirring conditions. Then, the filler was subjected to distilled water and filtered in order to remove the alkaline. This step was repeated in a count

of four times to assure substantial removal of the hemicellulose. The bleaching treatment was employed on the OPEFB fibre after it was dispersed in distilled water. The resultant OPEFB suspension was then bleached using the diluted NaClO_2 and mechanically stirred for 1 h at 80°C . The step was repeated three times to assure the removal of the lignin and hemicellulose. The treated fibre was subsequently washed with distilled water and filtered. The acid hydrolysis using 65% H_2SO_4 was conducted under stirring condition at a temperature of 45°C . The suspension of OPEFB was washed with cold distilled water in order to stop the reaction. The OPEFB suspension was then centrifuged at the speed of 7,500 rpm for about 15 min and this procedure was repeated for 10 times. The produced nanocellulose was homogenised for 30 s at 5,000 rpm before being dried in an oven at the temperature of 50°C for 24 h.

2.3 Chemical Treatment of OPEFB Nanoellulose using Formic Acid

This method was in accordance to Koay and Husseinsyah (2016).¹² The chemical treatment process was conducted by employing 3% (v/v) of formic acid which was dissolved in $\text{C}_3\text{H}_3\text{OH}$ and stirred. Then, OPEFB nanocellulose was added into the solution and stirred for a while. After stirring, the solution was left overnight. The next day, the treated OPEFB nanocellulose was filtered and dried in an oven at a temperature of 70°C .

2.4 Preparation of ACC Films

Prior to the dissolution of cellulose, the OPEFB nanocellulose and MCC were activated in the following solvents, firstly, in $\text{C}_3\text{H}_6\text{O}$ (for 1 h and dried in oven) followed by DMAC (for 1 h and dried in oven). This activation step was conducted to ensure the cellulose swell before the dissolution process. For the dissolution step, the activated OPEFB nanocellulose and MCC were dissolved in DMAC for 10 min. Next, LiCl at 8% (wt. vol^{-1}) was added to the mixture. The mixture was constantly stirred for 30 min until the LiCl completely dissolved in the solution. The cellulose solution was then poured onto a glass plate and left overnight. The next day, the resultant composite films were washed with distilled water to remove the residual of DMAC/LiCl before letting it dried at room temperature for a day.

2.5 Characterisation and Testing

2.5.1 Characterisation of the OPEFB nanocellulose

2.5.1.1 Transmission electron microscopy (TEM)

TEM model FEI TECNAI 20 was utilised to examine the morphology of the OPEFB nanocellulose. This analysis was also conducted to determine the size of the cellulose. The TEM procedure was conducted at SIRIM Kulim, Kedah. Prior to the imaging by TEM, the provided sample was sonicated in isopropanol to allow dispersion of the nanofiber. Without this process, the image of the nanocellulose could not be observed due to agglomeration of the cellulose particles. The magnification used was 97,000 \times .

2.5.1.2 Fourier transform infrared (FTIR)

Perkin Elmer spectrum FTIR spectrometer was used to analysis the functional groups of raw OPEFB fibre, OPEFB nanocellulose and formic acid-treated OPEFB nanocellulose. The wave number range was between 500 to 4,500 cm^{-1} . The spectra were recorded with 16 scans and resolution of 4 cm^{-1} .

2.5.2 Assessment on the properties, structure and morphology, moisture absorption and soil biodegradability of the ACC films

2.5.2.1 Tensile test

Instron Universal Testing Machine, model 5590, was used to conduct the tensile test which was based on ASTM D882. The cross-head speed of the testing was at 10 mm min^{-1} . Five replicates were tested for each sample. The mean values of the tensile strength, elongation at break and modulus of elasticity were recorded.

2.5.2.2 Microscopy characterisation

The scanning electron microscope (SEM), model JEOL JSM-6460LA was used to analyse the tensile fractured surface of the ACC films. The scan of SEM was run at the voltage of 10 and 20 kV. The samples were coated with a thin layer palladium to avoid charging, prior to imaging.

2.5.2.3 *Moisture absorption test*

Samples with the dimensions of 2 cm × 1.5 cm were prepared for water absorption test. The test was conducted at room temperature. The samples were first dried in an oven for 24 h at a temperature of 50°C. Prior to the test, the samples were weighed to determine their initial weight. At regular time (which is once a week), the weight of the humid film samples was recorded to determine the rate of absorption. The following equation was used to calculate the moisture absorption of the samples:

$$\text{Moisture absorption (\%)} = \frac{W_h - W_o}{W_o} \times 100 \quad (1)$$

W_h : weight of humid samples

W_o : initial weight of samples

2.5.2.4 *Soil biodegradability test*

This testing was conducted based on the procedure used by Laxmeshwar et al.,¹³ Koay and Husseinsyah,¹² and Zain, Wahab and Ismail.¹⁴ The ACC films were subjected to soil burial test for the duration of three months. The initial weight of the dry film samples was taken. The films with the size of 5 cm × 1.5 cm were buried in the soil by which the soil was sprayed with water once a week. The weight loss rate was calculated whereby the data was taken once a week by collecting the samples from the soil. Any soil and dirt on the films were removed. The samples were then dried in an oven at 50°C for 24 h before the films were weighed accordingly. The equation for determining the weight loss of the ACC films is as followed:

$$\text{Weight loss (\%)} = \frac{W_i - W_d}{W_i} \times 100 \quad (2)$$

W_i : initial weight of dry samples

W_d : dry weight of degraded samples

The weight loss rate indicates the biodegradation rate of the films.

3. RESULTS AND DISCUSSION

3.1 Morphology of OPEFB Nanocellulose and Characterisation of Untreated and Formic Acid-Treated OPEFB Nanocellulose

3.1.1 TEM of OPEFB nanocellulose

The TEM images of the untreated OPEFB nanocellulose can be observed in Figure 1. The TEM analysis revealed the presence of nano-size cellulose (nanocellulose) with the average size of about 10 nm in length. Nonetheless, the image showed that the nanocellulose appeared to be in agglomerated form. This can be related to the findings of Lani et al. who have indicated that the occurrence or development of agglomeration is as a result of the Van der Waals forces attraction that take place between the nanoparticles.¹⁵ This finding suggested that the extraction or isolation step of the OPEFB fibre led to the development of OPEFB nanocellulose.

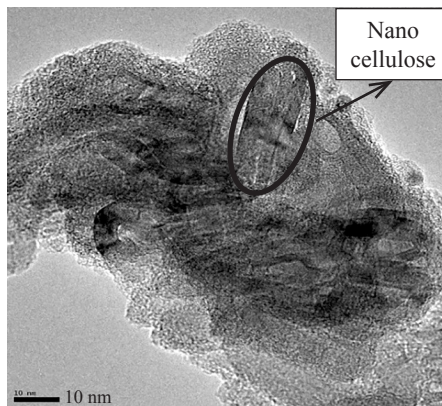


Figure 1: TEM image of the OPEFB nanocellulose at 97 k \times magnification.

3.1.2 Comparison on the FTIR analysis of the untreated and treated OPEFB nanocellulose

The FTIR spectra of untreated and formic acid-treated OPEFB nanocellulose are shown in Figure 2. The peak at $\sim 3,340\text{ cm}^{-1}$ for untreated nanocellulose and formic acid-treated nanocellulose reflect the stretching vibrations of $-\text{OH}$ group while the peaks between $2,888$ to $2,892\text{ cm}^{-1}$ are correlate to the stretching vibration of $\text{C}-\text{H}$ group.¹⁵⁻¹⁷ The sharp peaks at $1,036\text{ cm}^{-1}$ (untreated nanocellulose) and $1,039\text{ cm}^{-1}$ (formic acid nanocellulose) correspond to the $\text{C}-\text{O}-\text{C}$ pyranose ring stretching vibration in the nanocellulose.¹⁶

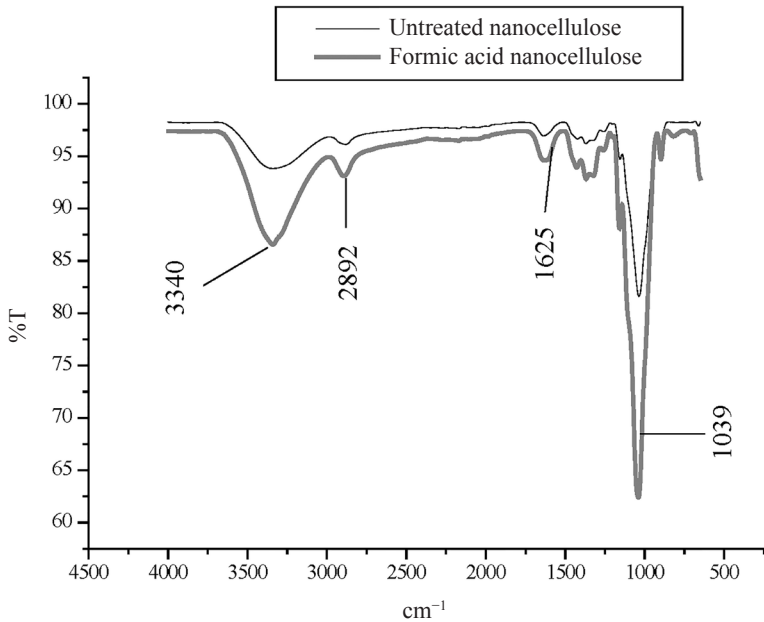


Figure 2: FTIR spectra of the untreated and formic acid-treated nanocellulose.

Moreover, the band at $1,625\text{ cm}^{-1}$ for formic acid-treated nanocellulose correspond to the characteristic of carbonyl group (-C=O).¹⁷ This can be associated with chemical treatment which resulted in the substitution of hydroxyl group (OH) from nanocellulose with the -C=O from the formic acid, respectively.¹⁷ The proposed molecular interaction between the nanocellulose and the formic acid is illustrated in Figure 3.

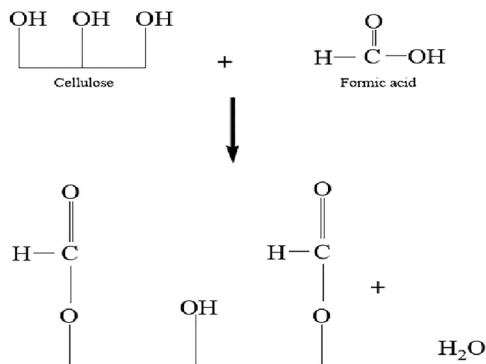


Figure 3: Proposed molecular interaction between the nanocellulose and formic acid.

3.2 Tensile Properties, Structure Morphology, Moisture Absorption and Soil Biodegradability of the ACC Films

3.2.1 Tensile strength

Figure 4 illustrates the tensile strength of the untreated and formic acid-treated ACC films containing OPEFB nanocellulose in 1%, 2%, 3% and 4% (wt. vol⁻¹) with uniform amount of MCC which is 3% (wt. vol⁻¹). The mean values of both untreated and treated composite films are shown in Table 1. Both composite films exhibit similar trend by which the tensile strength decreased as the contents of OPEFB increased from 1% (wt. vol⁻¹) to 4% (wt. vol⁻¹). The rise in OPEFB nanocellulose content led to cellulose aggregations which result in the dispersion of filler phase to be more difficult and complex throughout the matrix domain. This is due to the ACC films which also consist of the MCC, therefore the mixture of cellulose from both OPEFB and MCC led to the saturation of cellulose inside the films. It is important to mention that the addition of MCC in this study was to provide strengthening effect to the ACC films as previously recommended by Thirion.¹⁸ Preliminary work was done in which the ACC films were produced without the addition of MCC. Unfortunately, the ACC films produced were too brittle. This finding was also observed by Thirion.¹⁸ As MCC was added in constant amount (3% (wt. vol⁻¹)) in all the ACC films, the changes in the structure, morphology and properties of the ACC films reported in this work were assumed due to the OPEFB contents.

Apparently, the formic acid treatment of the nanocellulose enhanced the strength of the composite films containing 1%, 2%, 3% and 4 % (wt. vol⁻¹) of OPEFB nanocellulose. Among all the treated ACC films, the one containing 1% (wt. vol⁻¹) OPEFB nanocellulose exhibits the highest tensile strength at 25.1 MPa, by which the value increased by 214% as opposed to the untreated film at 1% (wt. vol⁻¹) of OPEFB content. The treated ACC films show greater tensile strength probably due to the chemical treatments that reduced the hydrogen bonds of the nanocellulose. The presence of $-C=O$ of the formic acid which substituted or replaced the OH of the nanocellulose, allows better dissolution of OPEFB nanocellulose in the solvent system, hence improve and enhance the interfacial adhesion between the matrix and fibre phase for better stress transfer mechanism. When the treated nanocelluloses were in contact with cellulose solvent (DMAC/LiCl), the solvent was allowed to partly dissolved the treated nanocellulose surface much easier because hydrogen bonds have been reduced.^{9,10} Therefore, better dissolution of the nanocellulose in the solvent can be achieved which can lead to enhancement of the interfacial interactions between the dissolved cellulose matrix and the non-dissolved cellulose fibre in the composite films.

Table 1: Tensile strength values of the untreated and formic acid-treated ACC films.

OPEFB contents % (wt. vol ⁻¹)	Untreated ACC films (MPa)	Formic acid-treated ACC films (MPa)
1	8.0 ± 0.4	25.1 ± 1.3
2	6.7 ± 0.3	13.3 ± 0.7
3	5.9 ± 0.3	9.7 ± 0.5
4	4.9 ± 0.2	7.1 ± 0.4

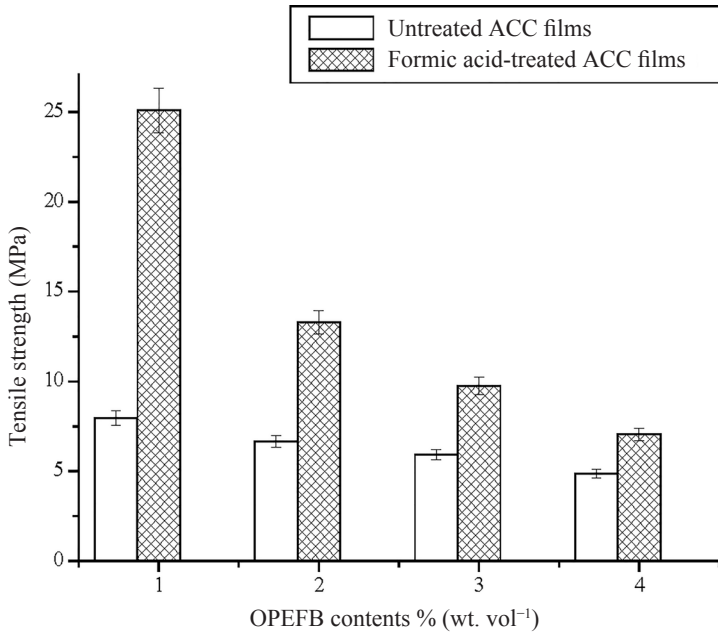


Figure 4: The effect of OPEFB nanocellulose contents on the tensile strength of the untreated and formic acid-treated ACC films.

A study by Govindan et al. on modified nypa fruticans regenerated cellulose biocomposite films using acrylic acid showed that the presence of acrylic acid has enhanced the tensile strength and Young's modulus of nypa fruticans regenerated cellulose biocomposite films compared to the unmodified films.¹⁹ Furthermore, Farah, Salmah and Marliza have conducted a research on the effect of butyl methacrylate on properties of regenerated cellulose coconut shell biocomposite films which showed that the treated biocomposite films with butyl methacrylate resulted in the improvement of the tensile strength, modulus of elasticity and crystallinity index (CrI) of the films.²⁰

However, it can be seen that the treated films demonstrated a reduction in the tensile strength when the OPEFB nanocellulose contents was higher than 1% (wt. vol⁻¹). This could be due to the agglomeration of the cellulose particles which derived from both MCC and OPEFB. This situation is in good agreement with the findings of Zailuddin et al.²¹

3.2.2 Elongation at break

Figure 5 displayed the effect of OPEFB nanocellulose contents on the elongation at break for both untreated and formic acid-treated ACC films at 3% (wt. vol⁻¹) of MCC and different OPEFB contents (1%, 2%, 3%, 4% (wt. vol⁻¹)). The mean values of elongation at break for both composite films are tabulated in Table 2. There is no compelling difference for the elongation at break values of both types of films when the OPEFB nanocellulose contents increased from 1% (wt. vol⁻¹) to 4% (wt. vol⁻¹).

Generally, in a conventional composite system, the presence of higher filler content would commonly increase the rigidity of the composite, thus reducing the elongation at break (flexibility) of the material. However, for this type of composite films the elongation at break results demonstrated no substantial changes. The elongation at break for the untreated films showed insignificant changes probably due to the surface area of the nanocellulose which were not high enough to generate large mechanical restrained especially when the interfacial interactions between the filler phases and matrix are feeble. Furthermore, it can be inferred that the amount of filler phase inside the matrix domain was not ample enough to allow substantial changes in the elongation at break of the ACC film even though the OPEFB contents increased to 4% (wt. vol⁻¹).

As for the formic acid-treated ACC films, the enhanced interfacial adhesion between the fibre and matrix domains should also improve and enhance the rigidity of the ACC films. Hence, lowering or decreasing the elongation at break values is expected. Nonetheless, the substitution of the OH group of the nanocellulose with the HCO group of the formic acid during the treatment has caused greater mobility in the polymer molecular chains, therefore the elongation at break value did not essentially change upon the chemical treatment. Moreover, this deformation performance of the ACC films also can be influenced by factors like absorption of moisture from the surrounding environment and incomplete dispersal of the fibre phase inside the matrix phase which can restrict stiffening of the films.

Table 2: Elongation at break values of the untreated and formic acid-treated ACC films.

OPEFB contents % (wt. vol ⁻¹)	Untreated ACC films (%)	Formic acid-treated ACC films (%)
1	12.2 ± 0.6	12.1 ± 0.6
2	12.3 ± 0.6	12.2 ± 0.6
3	12.5 ± 0.6	12.4 ± 0.6
4	13.1 ± 0.7	12.7 ± 0.6

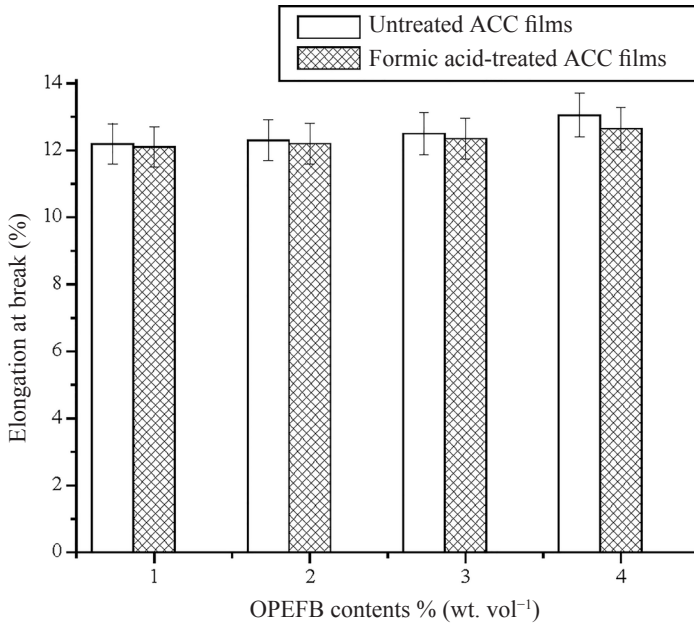


Figure 5: The effect of OPEFB nanocellulose contents on the elongation at break of the untreated and formic acid-treated ACC Films.

3.2.3 Modulus of elasticity

Figure 6 shows the modulus of elasticity of the untreated and formic acid-treated composite films incorporating OPEFB nanocellulose at various contents (1%, 2%, 3%, 4% (wt. vol⁻¹)) and constant amount of MCC (3% (wt. vol⁻¹)). Table 3 summarises the mean values of modulus of elasticity of the ACC films. The modulus of elasticity values of the untreated ACC films exhibit very small decrement when the OPEFB contents increased from 1% (wt. vol⁻¹) to 4% (wt. vol⁻¹). Inhomogeneous morphology of the untreated ACC films which consist

of incomplete cellulose dispersal may results in interference in load transfer efficiency, thus causing some reduction in its stiffness property, even though the OPEFB nanocellulose contents increased to 4% (wt. vol⁻¹). Besides that, the modulus of elasticity of the formic acid-treated ACC films showed a reduction trend when the OPEFB contents increased from 1% (wt. vol⁻¹) to 4% (wt. vol⁻¹). The reason for the decrement probably due to the saturation of the cellulose contents (OPEFB nanocellulose and MCC) that can lead to particles aggregation which result in their poor dispersion in the solvent. Eventually, lowering of the modulus occurred.

Table 3: Modulus of elasticity values of the untreated and formic acid-treated ACC films.

OPEFB contents % (wt. vol ⁻¹)	Untreated ACC films	Formic acid-treated ACC films
1	179.8 ± 9.0	606.6 ± 30.3
2	167.7 ± 8.4	563.4 ± 28.2
3	164.7 ± 8.2	314.3 ± 15.7
4	156.0 ± 7.8	235.8 ± 11.8

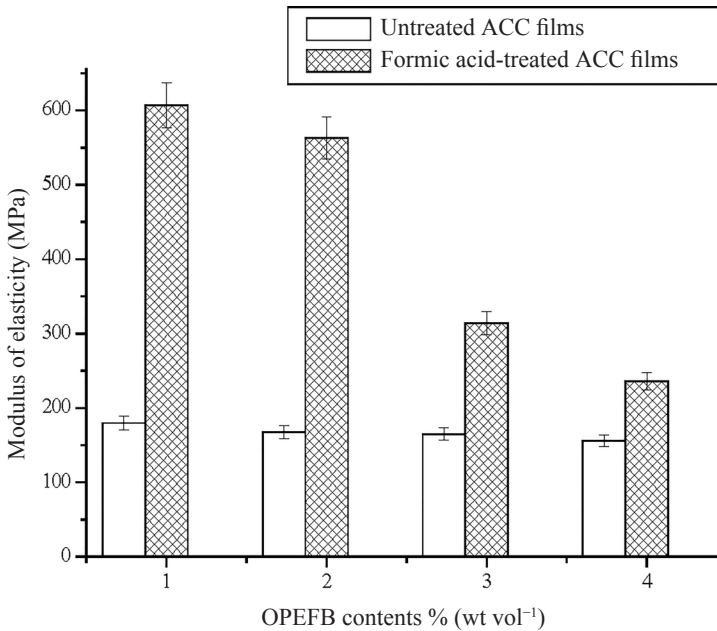


Figure 6: The effect of OPEFB nanocellulose contents on the modulus of elasticity of the untreated and formic acid-treated ACC Films.

The increase in OPEFB nanocellulose contents generates more cellulose aggregations which can result in difficulty in terms of cellulose dispersion. This can affect or influence the load transfer efficiency, hence decreasing the modulus. Among all the films, formic acid-treated ACC films at 1% (wt. vol⁻¹) of OPEFB content exhibit the highest modulus with the value of 606.6 MPa. The treated composite films exhibit better modulus of elasticity as opposed to the untreated films is presumably due to the OPEFB nanocellulose/MCC being well dispersed in the solvent system. The good interfacial interaction between the matrix phase and the filler phase contribute to a better or enhance filler distribution in the ACC films. A study by Govindan et al. showed that when the nypa fruticans was modified with acrylic acid, the regenerated cellulose biocomposite film possessed improved tensile strength and Young's modulus.¹⁹ Another research by Hahary et al. who studied the properties of ACC films from coconut shell powder and MCC showed that the addition of the coconut shell powder content in 3 wt. % has resulted in an increment of tensile strength and modulus of elasticity of the ACC film while elongation at break decreased.²⁰

3.2.4 SEM of the formic acid-treated ACC films

The SEM tensile fractured surface of both formic acid-treated ACC films at 1% and 4% (wt. vol⁻¹) OPEFB contents are shown in Figure 7(a) and (b). It can be observed from Figure 7(b) that the cluster of cellulose results in a rougher surface when 4% (wt. vol⁻¹) OPEFB was employed to produce the ACC film. However, for 1% (wt. vol⁻¹) OPEFB treated film, the micrograph demonstrates a smoother surface. This SEM analysis supports the tensile strength results whereby the treated films at 1% (wt. vol⁻¹) of OPEFB contents has higher tensile strength compared to the treated film at 4% (wt. vol⁻¹) of OPEFB content.

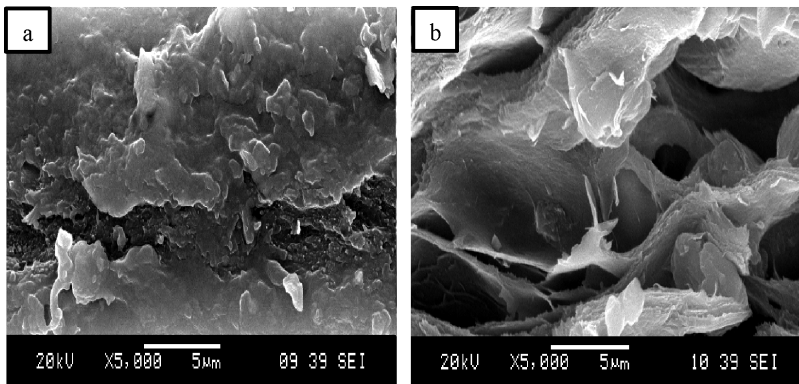


Figure 7: SEM micrographs of tensile fractured surface of formic acid-treated ACC films at (a) 1% (wt. vol⁻¹) OPEFB contents and (b) 4% (wt. vol⁻¹) OPEFB contents.

3.2.5 Moisture absorption of the ACC films

The moisture absorption of ACC films containing constant amount of MCC plus 1% (wt. vol⁻¹) and 4% (wt. vol⁻¹) of OPEFB contents are shown in Figure 8(a) and (b). This section of experiment is conducted within the time span of three months. It can be seen from Figure 8(a), between weeks 8th to 10th, formic acid-treated ACC film at 1% (wt. vol⁻¹) of OPEFB content, absorbed more moisture at about 10.56% to 21.13%, respectively. The reason for this is due to the structure of the treated cellulose with formic acid having no alkyl group like methyl (CH₃) attached as substituted group in the nanocellulose structure during the modification process. This alkyl group are known to be non-polar therefore they are considered to be hydrophobic. Since the treated film with formic acid does not consist of these functional groups, the molecular chains are more permeable to moisture/water.

Generally, when treatment is made to the cellulose, it will become more hydrophobic therefore attraction to moisture or water would be lower or decrease.²² In this study, the substitution or replacement of the –OH group of the nanocellulose with the functional groups of the formic acid treatment led to the reduction of hydrogen bonds. This results in the formation of more free volume within the cellulosic molecular chains which can allow higher degree of the moisture to be permeated inside the treated ACC films. Pang et al. explained in their article that the acetylation of cellulose causes the hydrogen bond to be partially destroyed and the appearance of lateral spaces between the long cellulose chains. Furthermore, the untreated films shrink to a considerate extend which result in a thicker film to be formed as opposed to the treated films. This consequently led to slow moisture absorption into the untreated films.²³ That is why formic acid-treated ACC film tends to absorb more moisture compared to the untreated composite films.

The ACC films containing 4% (wt. vol⁻¹) of the untreated OPEFB nanocellulose tend to absorb more moisture as compared to the ACC films with 1% (wt. vol⁻¹) of the untreated OPEFB nanocellulose. This phenomenon can be clearly observed on 13th week. This trend can be correlated with the findings of Lani et al. who suggested that the increase of nanocellulose content may enhance the water absorption rate because the aggregations of particles can form voids for the water molecules to diffuse in.¹⁵ The unsteady trends that the films illustrate during the whole 14 weeks could presumably due to the surrounding condition that could influence the absorption rate. The high moisture absorption rate that can be seen between ninth and 10th week could possibly due to the rise in the humidity due to the raining season.

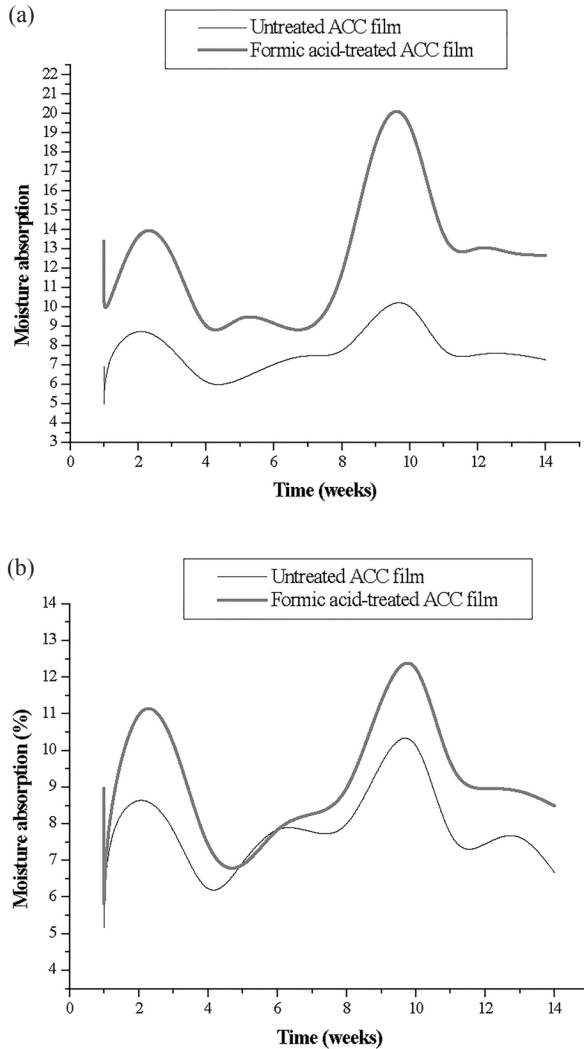


Figure 8: Moisture absorption of untreated and formic acid-treated ACC films at (a) 1% (wt. vol⁻¹) and (b) 4% (wt. vol⁻¹) of OPEFB contents.

3.2.6 Biodegradability of the ACC films

The biodegradability of the ACC films was assessed through the percentage of weight loss of the materials upon the measured time. Figure 9(a) and (b) illustrates the weight loss of ACC films in soil for the duration of three months. It can be seen that the weight loss rate for formic acid-treated ACC films at 1% (wt. vol⁻¹) of OPEFB contents is rather swift, which is 56.56% on the fourth week. This is then

followed by complete weight loss that happened on the following week. This can be related with the moisture absorption results by which the 1% (wt. vol⁻¹) OPEFB treated films with formic acid absorbed more moisture than 1% (wt. vol⁻¹) OPEFB untreated film. When more moisture is absorbed by the films, it will entice more microorganisms to grow and decompose the films.¹⁵ As a result, the formic acid treated ACC film degrades faster than the untreated ACC film.

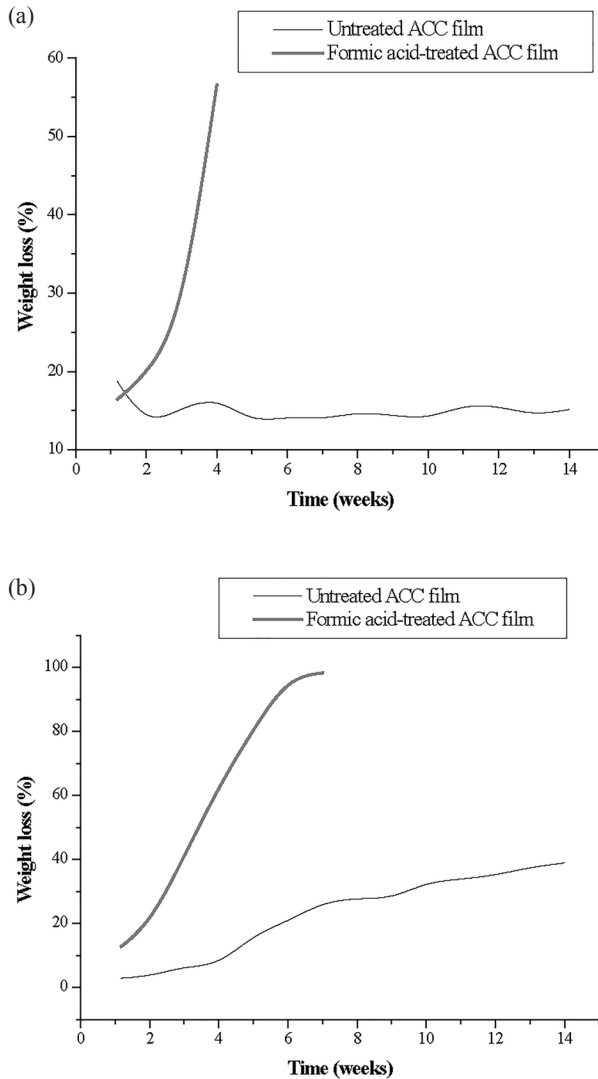


Figure 9: Weight loss of both untreated and formic acid-treated ACC films at (a) 1% (wt. vol⁻¹) and (b) 4% (wt. vol⁻¹) of OPEFB contents.

Furthermore, it can be observed in Figure 9(b) that the weight loss for both untreated and treated ACC films with 4% (wt. vol⁻¹) of OPEFB contents increased constantly until the end of the experiment. This is presumably due to the agglomerations of cellulose particles in the films which can leave voids between them, hence making excess for moisture from the soil to permeate efficiently into the films and subsequently increase the weight loss (biodegradation rate). This situation can be described further by Lani et al. whereby the fast disintegration of PVA/starch blend films is due to great amount of water the films absorbed which eventually results in microorganisms to attach and cultivate on the films.¹⁵

4. CONCLUSION

In this study, we have investigated the use of formic acid for chemical treatment of the OPEFB nanocellulose and analysed its efficiency to improve the tensile properties of the OPEFB cellulose-derived ACC film. Based on the FTIR spectra, it can be proved that the chemical treatment resulted in the substitution of OH from nanocellulose with the –C=O from the formic acid. This reduction in OH group of the cellulose assists in better dissolution of cellulose during the formation of the ACC film. Both treated and untreated ACC films show the highest value of tensile strength and modulus of elasticity when 1% (wt. vol⁻¹) of OPEFB was used to form the composite. However, both types of ACC films exhibit reduction in tensile strength and modulus of elasticity when the OPEFB content increased from 1% to 4% (wt. vol⁻¹). This could be due to cellulose particle aggregations and saturation that induced the formation of stress concentrated area along the composite structure. Nevertheless, the treated ACC films showed higher tensile strength and modulus of elasticity as compared to the untreated ACC films due to improved interfacial interactions between the dissolved cellulose matrix and the non-dissolved cellulose fibre in the biocomposite films. Furthermore, chemical treatment of the OPEFB nanocellulose using formic acid caused higher water absorption rate of the resultant ACC film. This subsequently induced greater biodegradation rate of the ACC films when buried in soil.

5. REFERENCES

1. Rong, S. Y., Mubarak, N. M. & Tanjung, F. A. (2017). Structure-property relationship of cellulose nanowhiskers reinforced chitosan biocomposite films. *J. Environ. Chem. Eng.*, 5(6), 6132–6136, <https://doi.org/10.1016/j.jece.2017.11.054>.

2. Reddy, K. O., Zhang, J., Zhang, J. & Rajulu, A. V. (2014). Preparation and properties of self-reinforced cellulose composite films from Agave microfibrils using an ionic liquid. *Carbohydr. Polym.*, 114, 537–545, <https://doi.org/10.1016/j.carbpol.2014.08.054>.
3. Osman, A. F., Ashafee, A. M. T. L., Adnan, S. A. & Alakrach, A. (2020). Influence of hybrid cellulose/bentonite fillers on structure, ambient and low temperature tensile properties of thermoplastic starch composites. *Polym. Eng. Sci.*, 60(4), 810–822, <https://doi.org/10.1002/pen.25340>.
4. Husseinsyah, S., Azmin, A. N. & Suppiah, K. (2016). Effect of eco-degradant on properties of recycled polyethylene (RPE)/chitosan biocomposites. *Journal of Engineering Science*, 12, 53–64.
5. Gopinath, V., Saravanan, S., Al-Maleki, A. R., Ramesh, M. & Vadivelu, J. (2018). A review of natural polysaccharides for drug delivery applications: Special focus on cellulose, starch and glycogen. *Biomed. Pharmacother.*, 107, 96–108, <https://doi.org/10.1016/j.biopha.2018.07.136>.
6. Zailuddin, N. L. I., Osman, A. F., Husseinsyah, S., Ariffin, Z. & Badrun, F. H. (2017). Mechanical properties and x-ray diffraction of oil palm empty fruit bunch all-nanocellulose composite films. In R. Saian & M. A. Abbas (eds.), *Proceedings of the Second international conference on the future of ASEAN (ICoFA) 2017: Volume 2; Science and technology*. Singapore: Springer, 505–514, https://doi.org/10.1007/978-981-10-8471-3_50.
7. Abdul Khalil, H. P. S., Jawaid, M., Hassan, A., Paridah, M. T. & Zaidon, A. (2012). Oil palm biomass fibres and recent advancement in oil palm biomass fibres based hybrid biocomposites. In N. Hu (ed.), *Composites and their applications*. London: IntechOpen, 187–220, <https://doi.org/10.5772/48235>.
8. Zaaba, N. F, Jaafar, M. & Ismail, H. (2017). The effect of alkaline peroxide pre-treatment on properties of peanut shell powder filled recycled polypropylene composites. *Journal of Engineering Science*, 13, 75–87, <https://doi.org/10.21315/jes2017.13.6>.
9. Huber, T., Mussig, J., Curnow, O., Pang, S., Bickerton, S. & Staiger, M. P. (2012). A critical review of all-cellulose composites. *J. Mater. Sci.*, 47, 1171–1186, <https://doi.org/10.1007/s10853-011-5774-3>.
10. Medronho, B. & Lindman, B. (2015). Brief overview on cellulose dissolution/regeneration interactions and mechanisms. *Adv. Colloid Interface Sci.*, 222, 502–508, <https://doi.org/10.1016/j.cis.2014.05.004>.
11. Dupont, A. (2003). Cellulose in lithium chloride/N-N-dimethylacetamide, optimization of a dissolution method using paper substrates and stability of the solutions. *Polymer*, 44(15), 4117–4126, [https://doi.org/10.1016/S0032-3861\(03\)00398-7](https://doi.org/10.1016/S0032-3861(03)00398-7).

12. Koay, S. C. & Husseinsyah, S. (2016). Agrowaste-based composites from cocoa pod husk and polypropylene. *J. Thermoplast. Compos. Mater.*, 29(10), 1332–1351, <https://doi.org/10.1177/0892705714563125>.
13. Laxmeshwar, S. S., Kumar, D. J. M., Viveka, S. & Nagaraja, G. K. (2012). Preparation and properties of composite films from modified cellulose fibre-reinforced with PLA. *Der. Pharma. Chem.*, 4(1), 159–168, <https://doi.org/10.5402/2012/154314>.
14. Zain, A. H. M., Wahab, M. K. A. & Ismail, H. (2018). Biodegradation behaviour of thermoplastic starch: The roles of carboxylic acids on cassava starch. *J. Polym. Environ.*, 26(2), 691–700, <https://doi.org/10.1007/s10924-017-0978-5>.
15. Lani, N. S., Ngadi, N., Johari, A. & Jusoh, M. (2014). Isolation, characterization, and application of nanocellulose from oil palm empty fruit bunch fiber as nanocomposites. *J. Nanomater.*, 2014, 1–9, <https://doi.org/10.1155/2014/702538>.
16. Soni, B., Hassan, E. B. & Mahmoud, B. (2015). Chemical isolation and characterization of different cellulose nanofibers from cotton stalks. *Carbohydr. Polym.*, 134, 581–589, <https://doi.org/10.1016/j.carbpol.2015.08.031>.
17. Ramli, S., Ja'afar, M. S., Sisak, M. A. A., Zainuddin, N. & Rahman, I. A. (2015). Formulation and physical characterization of microemulsions based carboxymethyl cellulose as Vitamin C carrier. *Malaysian J. Anal. Sci.*, 19(1), 275–283.
18. Thirion, C. (2015). All-cellulose composite production using an ionic liquid. MEng diss., University of Pretoria.
19. Govindan, V., Hussiensyah, S., Leng, T. P. & Amri, F. (2014). Preparation and characterization of regenerated cellulose using ionic liquid. *Adv. Environ. Biol.*, 8(8), 2620–2625.
20. Farah, N. H., Salmah, H. & Marliza, M. (2016). Effect of butyl methacrylate on properties of regenerated cellulose coconut shell biocomposite films. *Procedia Chem.*, 19, 335–339, <https://doi.org/10.1016/j.proche.2016.03.020>.
21. Zailuddin, N. L. I., Husseinsyah, S., Hahary, F. N. & Ismail, H. (2017). Characterization and properties of treated oil palm empty fruit bunch regenerated cellulose biocomposite films with butyl methacrylate using ionic liquid. *Polym. Plast. Technol. Eng.*, 56(2), 109–116, <https://doi.org/10.1080/03602559.2016.1146902>.

22. Babae, M., Jonoobi, M., Hamzeh, Y. & Ashori, A. (2015). Biodegradability and mechanical properties of reinforced starch nanocomposites using cellulose nanofibers. *Carbohydr. Polym.*, 132, 1–8, <https://doi.org/10.1016/j.carbpol.2015.06.043>.
23. Pang, J., Liu, X., Yang, J., Lu, F., Wang, B., Xu, F. et al. (2016). Synthesis of highly polymerized water-soluble cellulose acetate by the side reaction in carboxylate ionic liquid 1-ethyl-3-methylimidazolium acetate. *Sci. Rep.*, 6, 33725, <https://doi.org/10.1038/srep33725>.